27th ABCM International Congress of Mechanical Engineering
December 04-08, 2023, Florianópolis-SC, Brazil

COB-2023-1014
NUMERICAL STUDY OF THE BUOYANT DIFFUSION FLAMES STABILITY IN A RECTANGULAR GROOVE

Renan Batista Matheus Ferreira[a]
Jean Carlos Guedes Souza[a]
Fernando Fachini Filho[b]
Caio Guimarães Maioli[a]
Guilherme Gonçalves Alvarez[a]
Eduardo Reis Sampaio Filho[a]
Leandro Marochio Fernandes[a]
[a]Instituto Federal de Educação, Ciência e Tecnologia do Espírito Santo - Campus Cachoeiro de Itapemirim, Rodovia Engenheiro Fabiano Vivácqua, 1568 – Morro Grande | Cachoeiro de Itapemirim - ES | CEP: 29322-000 - Brazil
renanb.matheus@gmail.com
jeancarlosguedessouza03@gmail.com
caio.maioli@ifes.edu.br
guilherme.alvarez@hotmail.com
engmec.eduardorsf@gmail.com
leandro.mfernandes@ifes.edu.br
[b]Grupo de Mecânica de Fluidos Reativos, Coordenação de Pesquisa Aplicada e Desenvolvimento Technologico - COPDT, Instituto Nacional de Pesquisas Espaciais INPE, 12630-000 Cachoeira Paulista/SP, Brazil
fachiniff@gmail.com

Abstract. *The objective of this work is to study numerically the transient behavior of buoyant diffusion flames in a rectangular groove, in which the fuel is methane. The simulations are performed using the fireFOAM solver, included in OpenFOAM, because it describes very well reacting flow driven by buoyancy. The instability of buoyant diffusion flames is a classic problem arising from the formation of vortices at the base of the flame. These vortices are generated by the difference in velocities in the shear layer at the base of the flame. In addtion, the natural convection increases the intensity of the vortices, carries them to the flame tip, and augments their radii. Depending on the height of the flame, flickering may occur. Flickering is the oscillatory movement of the flame tip caused by the passage of vortices. Most of the studies already carried out in this issue involve flames with axisymmetric geometry. At the present analysis, the flame geometry is imposed by a rectangular groove. The groove geometry allows a two-dimensional analysis and symmetric condition is imposed. The simulation results capture the physics of the phenomenon in question: the shape of the flame, the oscillation frequency, and the vortices dynamics.*

Keywords: *groove, flickering, buoyant diffusion flames.*

1. INTRODUCTION

The instability of buoyant diffusion flames is a classic problem arising from the formation of vortices at the base of the flame. These vortices are generated by the difference in velocities in the shear layer at the base of the flame. The natural convection, typical of combustion with very low velocity, increases the intensity of the vortices, and displaces them towards to the tip of the flame. During the displacement, the vortices augment their radii. Depending on the height of the flame, the effect of the vortices can impose an oscillation to the flame tip (flickering phenomenon) or divide the flame in two (puffing phenomenon). In this work, the flickering is analyzed.

Flickering is the oscillatory movement of the flame tip caused by the passage of vortices and puffing is the flame squeezing which leads to a local extinction and a pocket flame is separated from the main flame and transported away. According to Xia and Zhang (2018), flickering is a periodic phenomenon. The oscillation frequency associated with flickering is proportional to the inverse of the square root of the burner diameter. The fluid dynamic phenomenon that triggers this oscillatory behavior was studied by Buckmaster and Peters (1988) when analyzing the stability of an infinite candle model. The cause of the oscillation was attributed to the Kelvin-Helmholtz instability induced by buoyancy. Chen *et al.* (1989) visualized laminar jet diffusion flame flow and identified two types of vortices. The small ones inside the flame is induced by the Kelvin-Helmholtz instability, and the large ones outside the flame is induced by the Rayleigh–Taylor instability. These instabilities change the flame shape.

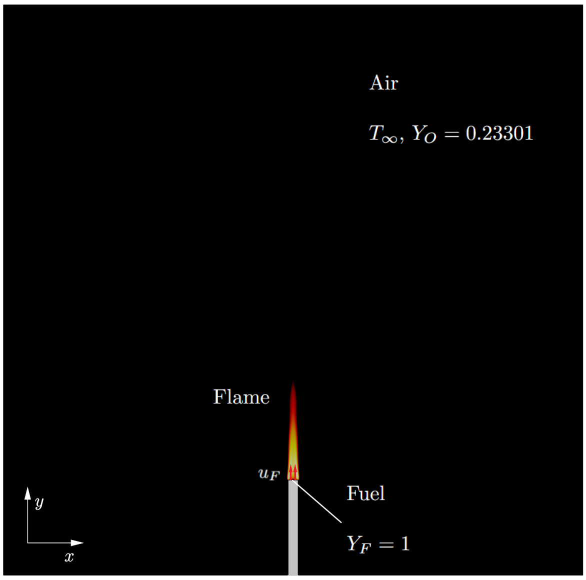

Figure 1. Case representation.

The shape of diffusion flames as well as theories to describe their behavior have been studied for a long time, such as Burke and Schumann (1928), who analyzed a burner with axisymmetric geometry. They studied the influence of velocity, temperature and species fields on the shape of the flame. Chamberlin and Rose (1928) in turn quantitatively investigated flickering, where the flame was located in a burner with square geometry. They estimate the flickering frequency using experimental analysis. There is an influence of the geometry and dimensions of the burner on the oscillation of the flame, according to Durao and Whitelaw (1974), who observed correlations between the intensity of the oscillations and the dimensions of the burner.

Considering that most works use axisymmetric burners, the present work has the objective of numerically studying the instability of diffusion flames in a rectangular groove. The groove geometry allows a two-dimensional analysis and symmetric condition is imposed to reduce even more the computational cost. No pyrolysis and soot chemistry were considered. In this work, the infinite-fast chemistry combustion model is assumed. The Reynolds number, based on the groove width and fuel velocity or the air flow imposed by the buoyancy, shows that the flow is in the laminar regime. Once the velocity and temperature fields are obtained, a fast Fourier transform can be applied to estimate the predominant oscillation frequency.

2. METHODOLOGY

The numerical analysis used the fireFOAM solver, which is part of OpenFOAM, an open source C++ library for computational fluid dynamics, which captures very well the dynamics of reactive flows driven by buoyancy. The conservation equations are solved numerically based on a finite volume scheme.

2.1 Case Description

The problem under investigation is represented in Fig. 1, showcasing an infinite-length groove burner. The burner has a thickness of $l_c = 0.015\ m$, and a height of $10l_c$. Methane is utilized as the fuel.

The chemical species involved follow the following combustion equation, in mass units:

$$CH_4 + 4O_2 \longrightarrow 5P, \tag{1}$$

Fuel and oxidant do not coexist outside the reaction sheet, characterizes a non-premixed regime. Assuming that the flame appears as a thin sheet of reaction, the chemical time scale is infinitely small and thus $Da >> 1$. No pyrolysis and soot chemistry were considered. The fuel inlet velocity is imposed as $u_F = 0.01\ m/s$ being the laminar flow. The air flow is generated by the buoyant force induced by the density stratification caused by the flame.

2.2 Flow equations

The nondimensionalized conservation equations for mass, momentum, energy and species are:

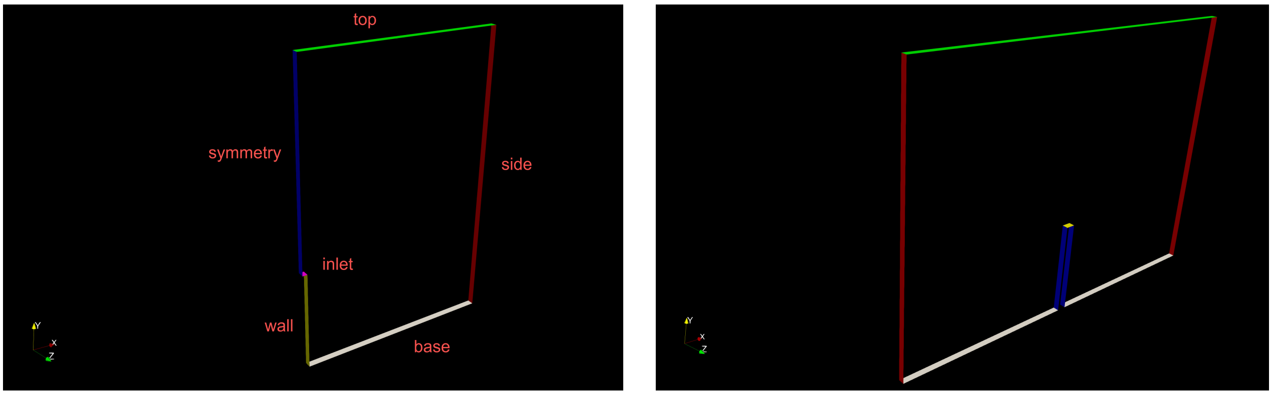

Figure 2. Case boundaries and reflection on the axis of symmetry.

$$St\frac{\partial \rho}{\partial t} + \nabla \cdot \rho \mathbf{v} = 0 \tag{2}$$

$$St\frac{\partial \rho \mathbf{v}}{\partial t} + \nabla \cdot \rho \mathbf{v}\mathbf{v} = -\frac{1}{\gamma Ma^2}\nabla p + \frac{1}{Re}\nabla \cdot \bar{\bar{\tau}} + \frac{1}{Fr^2}(1-\rho)\mathbf{e}_y \tag{3}$$

$$St\frac{\partial \rho T}{\partial t} + \nabla \cdot \rho \mathbf{v} T = \frac{1}{Pe}\nabla \cdot (k\nabla T) + \frac{\gamma - 1}{\gamma}\mathbf{v}\cdot \nabla p + \frac{Ec}{Re}\Phi + QDa\dot{\omega} \tag{4}$$

$$St\frac{\partial \rho Y_i}{\partial t} + \nabla \cdot \rho \mathbf{v} Y_i = \frac{1}{PeLe_i}\nabla \cdot (\rho D_i \nabla Y_i) + s_i Da\dot{\omega} \tag{5}$$

in which the independent and dependent variables are defined as

$$t = \frac{\hat{t}}{\hat{t}_c},\ x = \frac{\hat{x}}{\hat{l}_c},\ y = \frac{\hat{y}}{\hat{l}_c},\ \rho = \frac{\hat{\rho}}{\hat{\rho}_c},\ \mathbf{v} = \frac{\hat{\mathbf{v}}}{\hat{V}_c},\ p = \frac{\hat{p}}{\hat{p}_c},\ T = \frac{\hat{T}}{\hat{T}_c},\ Y_O = \frac{\hat{Y}_O}{\hat{Y}_{O\infty}},\ Y_F = \frac{\hat{Y}_F}{\hat{Y}_{F0}}$$

and the parameters are defined as

$$St = \frac{\hat{t}_c}{(\hat{l}_c/\hat{V}_c)},\quad Ma = \frac{\hat{V}_c}{\hat{a}},\quad Re = \frac{\hat{l}_c\hat{V}_c}{\hat{\nu}},\quad Fr^2 = \frac{\hat{V}_c^2}{\hat{g}\hat{l}_c},\quad Q = \frac{\hat{Q}}{(\hat{c}_p\hat{T}_c)},$$

$$Pe = \frac{\hat{l}_c\hat{V}_c}{\hat{\alpha}_c},\quad Le_i = \frac{\hat{\alpha}_c}{\hat{D}_{ic}},\quad Ec = \frac{\hat{V}_c^2}{(\hat{c}_p\hat{T}_c)},\quad Da = \frac{\hat{l}_c}{\hat{V}_c}B\hat{Y}_{O\infty}^{a_1}\hat{Y}_{F0}^{a_2}e^{-\hat{E}_a/(\hat{R}\hat{T}_c)}.$$

According to the chemical reaction $s_F = -1$, $s_O = -4$ and $s_P = 5$.

The subscript represent $i = F$ for fuel and $i = O$ for oxidant. $\hat{\rho}$, $\hat{\mathbf{v}}$, $\hat{p}$, $\hat{T}$ and $\hat{Y}$ are the specific mass, velocity, pressure, temperature and mass fraction of the gaseous mixture, respectively. $\hat{g}$ is the gravity acceleration, $\dot{\hat{\omega}} = \hat{\rho}BY_O^{a_1}Y_F^{a_2}\exp(-\hat{E}_a/(\hat{R}\hat{T}))$ (B is frequency factor, $\hat{R}$ is constant of gases, and $\hat{E}_a$ is the activation energy) is the reaction rate, $\hat{Q}$ is the heat released by combustion and radiation, $\hat{\Phi}$ is the dissipation function defined as $\hat{\Phi} = \hat{\bar{\bar{\tau}}} : \hat{\nabla}\hat{\mathbf{v}}$ and $\hat{\bar{\bar{\tau}}}$ is the viscous stress tensor defined as $\hat{\bar{\bar{\tau}}} = \hat{\mu}(\hat{\nabla}\hat{\mathbf{v}} + \hat{\nabla}\hat{\mathbf{v}}^T)$. $\hat{\mu}$, $\hat{\alpha}$, $\hat{D}_i$ and $\hat{c_p}$ (dynamic viscosity, thermal diffusivity, species diffusivity and constant pressure specific heat) are functions of the temperature.

2.3 Numerical Method

The governing equations are numerically solved using OpenFOAM, employing a cell-centered unstructured finite volume scheme.

To enhance computational efficiency, a symmetric condition is imposed on the geometry. Figure 2 illustrates the case boundaries, with a reflection on the axis of symmetry.

The structured mesh consists of 144,720 hexahedral elements and has been specifically adapted to achieve a higher concentration of elements in the flame region. These elements exhibit a non-orthogonality value of 0, an skewness value

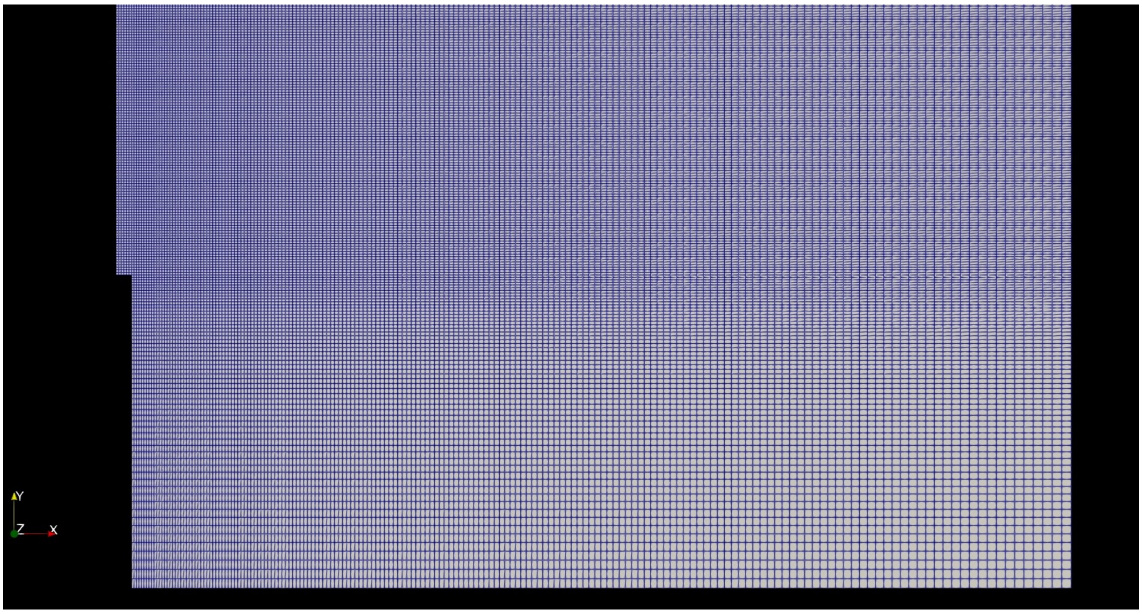

Figure 3. Zoomed-in view of the fuel inlet region.

tending to 0 (4.43788×10^{-13}) and a low maximum aspect ratio value (4.00705), the value being equal to 1 in the flame region. Figure 3 displays a zoomed-in view of the fuel inlet region.

Numerical schemes for terms are defined as follows: 'Euler' scheme is used for time derivatives, the 'Gauss linear' scheme is used for gradient derivative terms, the numerical scheme used to discretize the convective part in the species transport equation is 'limitedLinear01 1' which combines linear and upwind schemes. The pressure equation is solved by a linear GAMG solver and the PIMPLE algorithm is used for pressure-velocity coupling.

2.4 Boundary Conditions

The following boundary conditions are imposed: at the top, side and base, zero gradient is imposed for velocity, static pressure, temperature and fuel mass fraction of fuel and oxidant. At the inlet, a vertical velocity of 0.01 m/s, a temperature of 300 K, gradient zero for the static pressure, 1 for the mass fraction of fuel and 0 for the mass fraction of oxidant are imposed. On the wall, the zero gradient of all variables is imposed except for velocity, for which a no-slip condition is imposed. For symmetry, the symmetry condition is imposed on all variables. The initial field is given by 0 m/s for velocity, 300 K for temperature, 101325 kg/ms^2 for static pressure, 0 for the mass fraction of fuel and 0.23301 for the mass fraction of oxidant.

2.5 Post Processing

At the end of the simulation, using the ParaView utility, the fields of interest of the analyzed problem can be extracted. The flame oscillation frequency will be obtained by applying a fast Fourier transform in the temperature and velocity field. The region chosen to build the temperature graphs should be as close as possible to the occurrence of flickering. The fast Fourier transform was done using the GNU Octave software.

3. RESULTS AND DISCUSSIONS

The simulation was made to capture 10 seconds of the phenomenon. The results for the vertical velocity field and streamlines are shown in Fig. 4. It is observed that the central line of the groove has a higher speed due to density and species gradients. The surrounding air is moved by the buoyant force. Thus, its velocity is considerably lower than the velocity of the combustion products in central line.

For the horizontal velocity in Fig. 5 we can see the formation of vortices that move axially along the center line of the groove. The development of these vortices promotes oscillation. For the width used in the groove, there was not enough time for the vortices to grow to the point of strangling the flame. Therefore, no puffing phenomenon was observed. The natural flow of air entering the sides of the domain can be observed. This flow highlights the horizontal diffusive transport of oxidant to the flame, causing the flame to burn in a smaller region. As a symmetry condition was applied in the study, the left and right vortices do not interact with each other.

The results for the temperature field are show in Fig. 6.

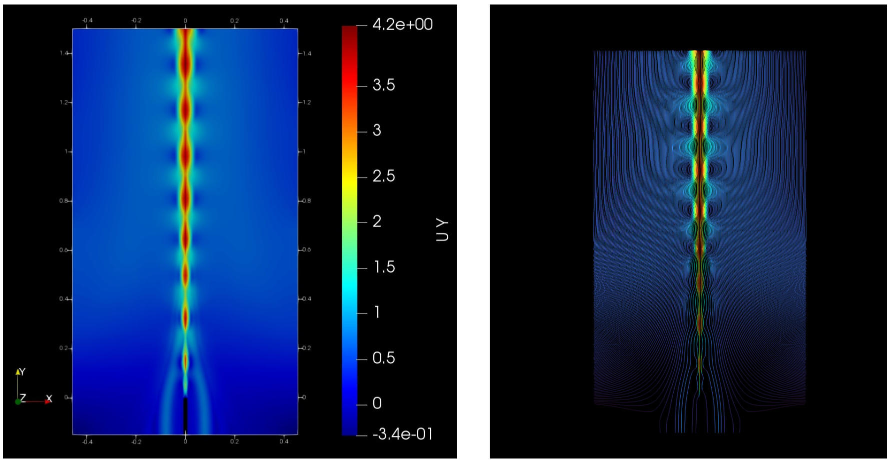

Figure 4. Speed U_y (m/s) and Streamlines at $t = 5$ s.

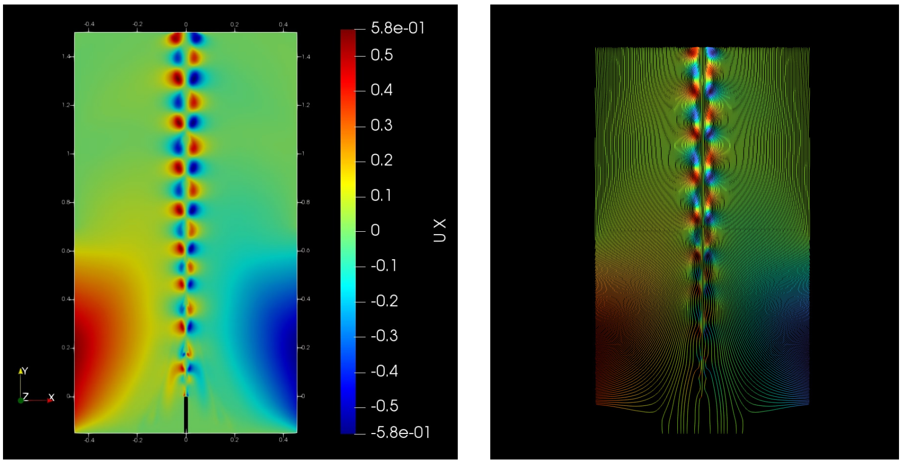

Figure 5. Speed U_x (m/s) and Streamlines at $t = 5$ s.

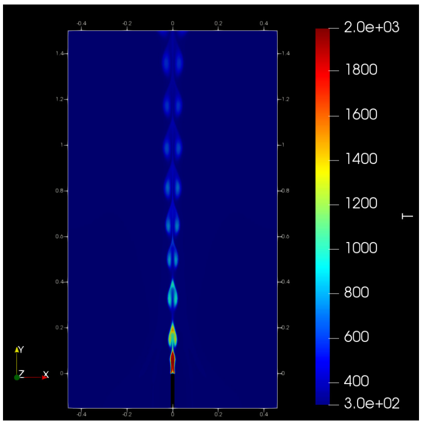

Figure 6. Temperature Field T (K) at $t = 5$ s.

To estimate the flickering frequency, it is first necessary to select the region of occurrence and plot the average velocity or temperature as a function of time. Through external software, a fast Fourier transform is applied to obtain the frequency spectrum and thus estimate the flame oscillation rate. Selecting a region located 15 cm above the groove, the velocity and temperature field are plotted as a function of time, according to Fig. 7 and Fig. 8.

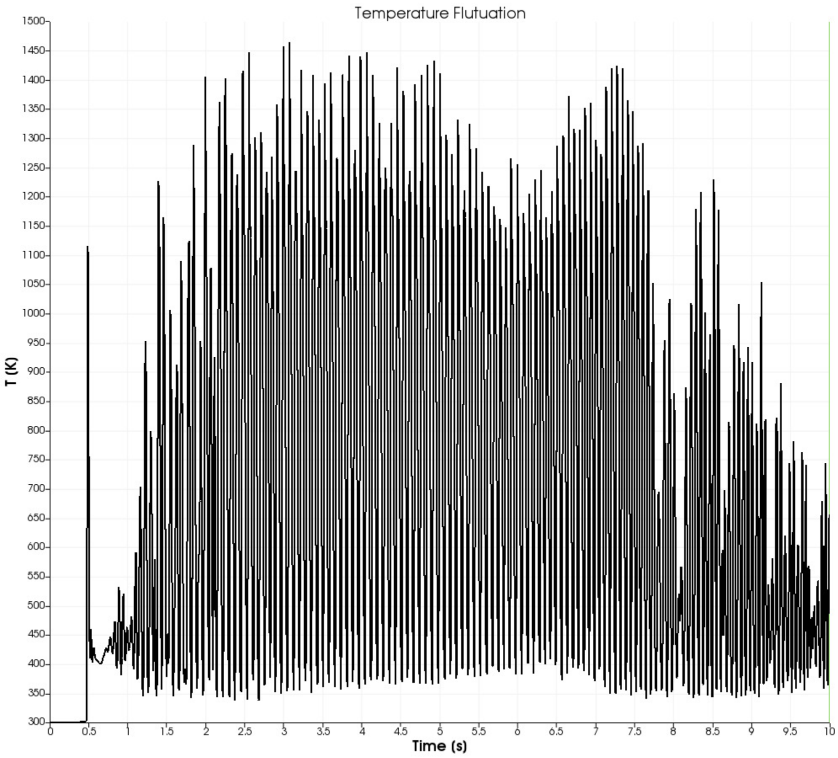

Figure 7. Temperature fluctuation over time in a region 15 cm above the groove.

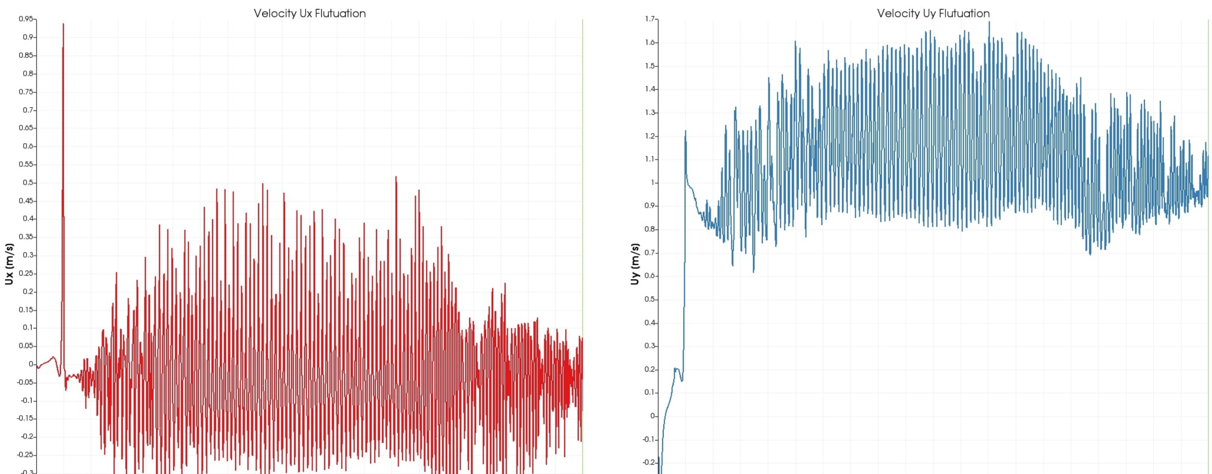

Figure 8. Speed U_x and U_y fluctuation over time in a region 15 cm above the groove.

Flickering is caused by the arising of vortices at the base of the flame. These vortices displaces to the top of the flame. The oscillation frequency of a diffusive flame varies in a range of 10 Hz to 20 Hz (Chamberlin and Rose, 1928; Buckmaster and Peters, 1988). Applying the fast Fourier transform, at the temperature, speed U_x and U_y we have the following spectrum of frequencies as shown in Fig. 9, Fig. 10 and Fig. 11.

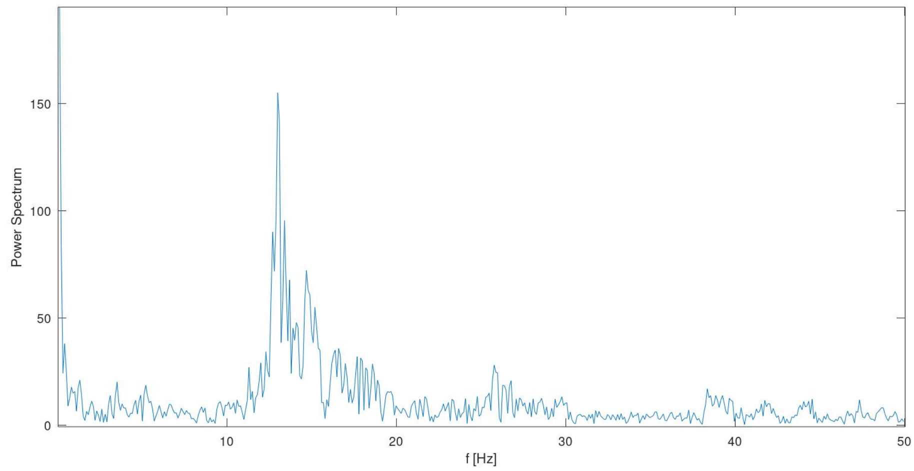

Figure 9. Oscillation frequency obtained from the temperature measurements. The frequency is $12.992\ Hz$.

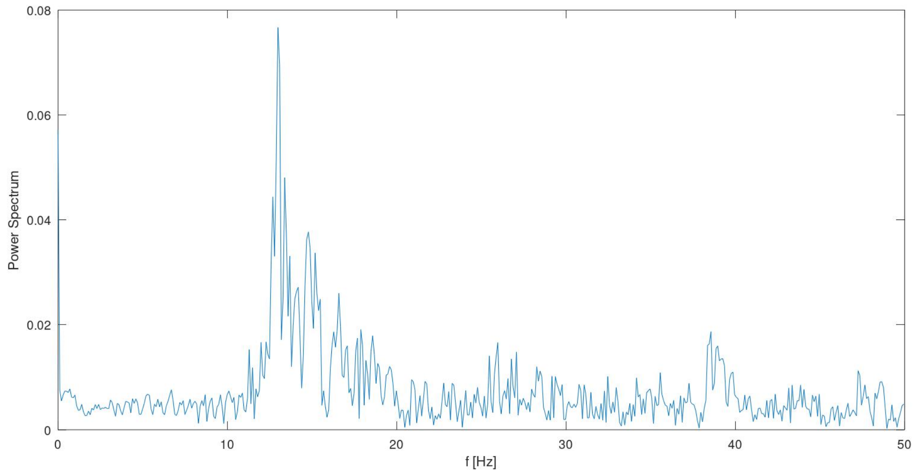

Figure 10. Oscillation frequency obtained from the x component of the velocity. The frequency is $12.984\ Hz$.

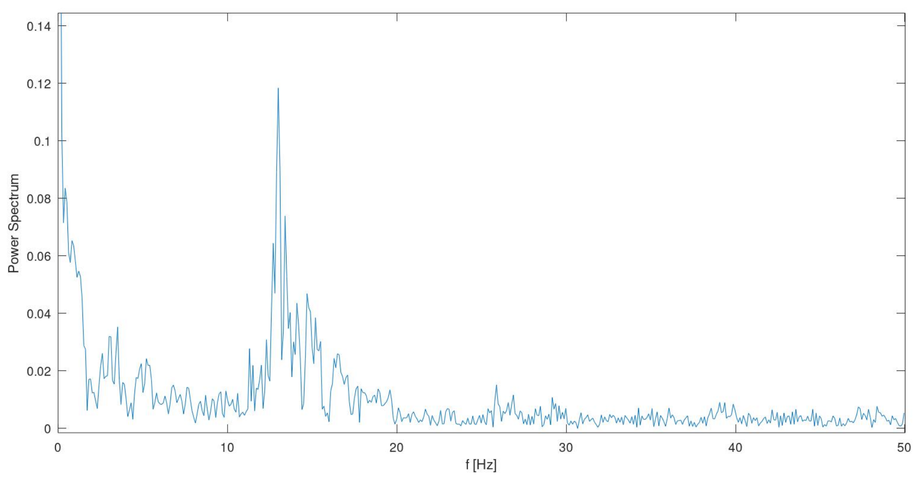

Figure 11. Oscillation frequency obtained from the y component of the velocity. The frequency is $12.972\ Hz$.

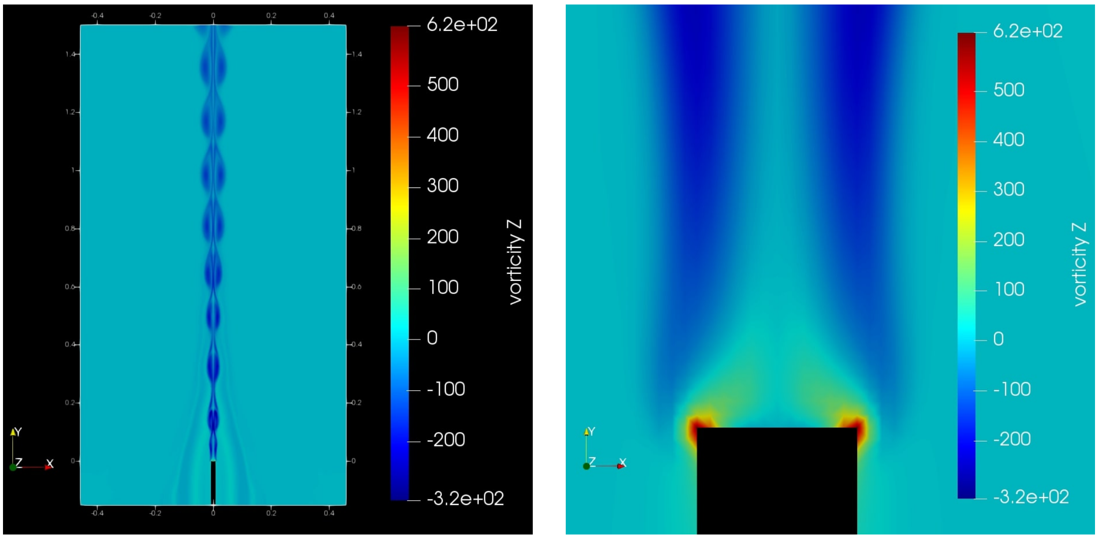

Figure 12. Vorticity Field $(1/s)$ at $t = 5$ s and Zoomed-in view of the fuel inlet region.

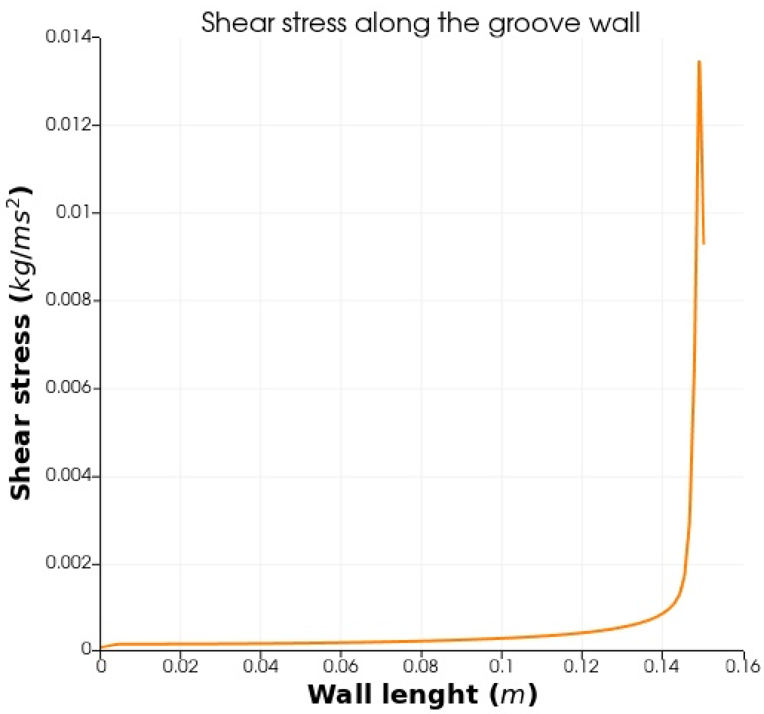

Figure 13. Shear stress (kg/ms^2) along the groove wall.

In Fig. 9, Fig. 10 and Fig. 11 is observed main frequency of 12.982 Hz, in concordance to the experimental results (Chamberlin and Rose, 1928; Buckmaster and Peters, 1988). Note that for any of the chosen properties, the obtained oscillation frequency is practically the same.

In addition to the main frequency in the 13 Hz range, we have some peaks of lesser intensity in the harmonics near 26 Hz and 39 Hz.

In Fig. 12 the vorticity field is shown, at the base of the flame it is possible to observe a vorticity peak. These vortices arise at the base of the flame as this is where the contact of air and fuel flows occurs. As the reagents are not previously mixed, their flows have different velocities, that generates vorticity.

Figure 13 such shows the shear stress along the groove wall. The shear peak occurs in the upper region of the channel, that coincides with the vorticity peak.

It is these vortices generated by the difference in velocities between reactants at the base of the flame that are axially convected by the flow and that generate part of the observed instabilities.

Residuals are extracted to verify the simulation results. The simulation produced residuals of the following orders of magnitude: 10^{-5} for fuel mass fraction, 10^{-3} for oxidant mass fraction, vertical velocity and temperature, ranging from 10^{-3} to 0.01 for horizontal velocity and between 0.01 and 0.1 for static pressure. These orders of magnitude are close to those observed in the tutorial cases of the fireFOAM solver. The solver, in turn, was validated in the work done by Wang *et al.* (2011).

4. CONCLUSION

The oscillation frequency associated with flickering depends on burner geometry. The fluid dynamic phenomenon that triggers this oscillatory behavior is associated with the Kelvin-Helmholtz instability and Rayleigh–Taylor instability that are induced by buoyancy. These instabilities change the shape of the flame. The results for the flame oscillation frequency showed a main frequency of 12.982 Hz, in agreement with experimental results that say that the oscillation frequency of a diffusive flame varies in a range of 10 Hz to 20 Hz. In addition to the main frequency in the 13 Hz range, we have some lower intensity peaks in the harmonics close to 26 Hz and 39 Hz. Note that for any property analyzed the value obtained for the oscillation frequency is practically the same.

Specialized literature has worked with burners with cylindrical geometry. The present research has attempted to provide analyzes regarding diffusive flames in groove geometry burners. The results obtained were then compared with data referring to burners with another geometry and are in the same order of magnitude. Studies carried out by the reactive thermofluid dynamics group have attempted to encompass the study of flames in grooves from the numerical to the experimental part to understand the influence of the burner geometry on the shape of the flame. One of the works of this group showed agreement regarding the values of the oscillation frequency for groove geometry.

5. ACKNOWLEDGEMENTS

The authors would like to acknowledge the academic support from Instituto Nacional de Pesquisas Espaciais (INPE) and the financial and academic support from Instituto Federal do Espírito Santo (IFES).

6. REFERENCES

Buckmaster, J. and Peters, N., 1988. “The infinite candle and its stability - a paradigm for flickering diffusion flames”. *Symposium (International) on Combustion*, Vol. 21, No. 1, pp. 1829–1836. ISSN 0082-0784. doi: https://doi.org/10.1016/S0082-0784(88)80417-X. Twenty-First Symposuim (International on Combustion).

Burke, S.P. and Schumann, T.E.W., 1928. “Diffusion flames”. *Industrial & Engineering Chemistry*, Vol. 20, No. 10, pp. 998–1004. doi:https://doi.org/10.1016/S0082-0784(88)80417-X.

Chamberlin, D.S. and Rose, A., 1928. “The flicker of luminous flames”. *Industrial & Engineering Chemistry*, Vol. 20, No. 10, pp. 1013–1016. doi:https://doi.org/10.1021/ie50226a009.

Chen, L.D., Seaba, J., Roquemore, W. and Goss, L., 1989. “Buoyant diffusion flames”. *Symposium (International) on Combustion*, Vol. 22, No. 1, pp. 677–684. ISSN 0082-0784. doi:https://doi.org/10.1016/S0082-0784(89)80075-X.

Durao, D.F.G. and Whitelaw, J.H., 1974. “Instantaneous velocity and temperature measurements in oscillating diffusion flames”. *Proceedings of the Royal Society of London. Series A, Mathematical and Physical Sciences*, Vol. 338, No. 1615, pp. 479–501. ISSN 00804630. URL `https://www.jstor.org/stable/78594`.

Wang, Y., Chatterjee, P. and de Ris, J.L., 2011. “Large eddy simulation of fire plumes”. *Proceedings of the Combustion Institute*, Vol. 33, No. 2, pp. 2473–2480. ISSN 1540-7489. doi:https://doi.org/10.1016/j.proci.2010.07.031.

Xia, X. and Zhang, P., 2018. “A vortex-dynamical scaling theory for flickering buoyant diffusion flames”. *Journal of Fluid Mechanics*, Vol. 855, p. 1156–1169. doi:https://doi.org/10.1017/jfm.2018.707.

7. RESPONSIBILITY NOTICE

The authors are the only responsible for the printed material included in this paper.